PROCEEDINGS OF THE INTERNATIONAL CONFERENCE NANOMATERIALS: APPLICATIONS AND PROPERTIES
Vol. **2** No 2, 02FNC08(3pp) (2013)

Nucleation and Growth of the Zn-Fe Alloy from a Chloride Electrolyte

S. Amirat[1,*], R. Rehamnia[1], R. Bensalem[1], M. Bordes[2], J. Creus[2]

[1] *Université Badji Mokhtar, BP 12, Annaba, Algeria*
[2] *Université de la Rochelle, FR-EDD CCA, Av. Michel Crépeau, F-17042 La Rochelle cedex 01, France*

(Received 20 May 2013; published online 31 August 2013)

In this study, the kinetics of Zn-Fe codeposition was investigated in chloride acidic solution using cyclic voltammetry. Anomalous codeposition is detected and this mechanism depends on the Zn(II) / Fe(II) concentration ratio in the electrolytic bath. The study of early stages of electrodeposition showed that Zn-Fe follows a theoretical response to instantaneous nucleation evolves into a progressive nucleation according to the model of Scharifker and Hills. The morphology and structure of the coatings is discussed using characterization techniques. Dense, uniform, and singlephased Zn-Fe coatings could be obtained with a Zn-Fe ratio of 1/3.

Keywords: Zn-Fe alloy, Chloride electrolyte, Electrocrystallisation, Cyclic voltammetry, SEM, XRD.

PACS numbers: 68.55. – a, 61.05.C –

1. INTRODUCTION

Zinc coatings are widely used for the protection of steel structures in industry but the application conditions are more and more severe that implies an improvement of the protective and functional properties of Zn coatings. During the last decades, zinc alloys were studied in order to improve the corrosion resistance or the mechanical properties of zinc-based coatings [1-9].

Among the electrodeposited zinc alloys, Zn-Fe electrodeposited coatings present many excellent properties, such as excellent corrosion resistance (due to the nature of the zinc-iron phases), good paintability, good welding [10], and it has been considered to be an alternative for pure zinc coating for the corrosion protection of steel products [11, 12]. Many techniques and studies were developed so as to improve the characterization of material surface reactivity and properties [13-16]. Zn-Fe alloys containing approximately 15-25 wt % of iron has been reported to present excellent corrosion resistance. These deposits were mainly synthesized from acidic sulfate or chloride electrolytic baths [17, 18].

The first stage of the formation of a new phase on a different substrate is generally accepted by the nucleation and growth process three-dimensional (3D), and also by adsorption reactions and the formation of low-dimensional systems: localized preferentially heterogeneous surfaces of substrates [19].

According to the model Sharifker and Hills it is possible to identify two types of nucleation: progressive and instantaneous in the case of a 3D germination and sprout growth controlled by diffusion.

The objective of the present work is to determine the shape of the crystal growth, supported by morphological information.

2. EXPERIMENTAL PROCEDURE

Electrodeposition was realized in a conventional glassy cell in stirred and aerated conditions. The bath composition and deposition parameters for the Zn-Fe deposits are: $ZnCl_2$ 0.15 mol/L,$FeCl_2$ 0.75 mol/L, Boric acid 25 g/L, Ascorbic acid 0.02 mol/L, pH 2, Temperature 25 °C, Current density (j) 10-50 mA/cm², Anode: Zn. All the chemicals are of high purity and the solutions were prepared using ultra-pure water (MilliQTM). Low alloy steel (steel 1.0037) cylinders were used as substrate and before electrodeposition, the samples were polished, degreased, and activated by dipping in a 50 vol % hydrochloric acid solution during 30 s. Then, samples were rinsed with ultrapure water and dried with fresh air.

The electrochemical characterization of the oxydo-reduction mechanisms occurring on the steel substrate electrode was performed using a conventional three electrodes potentiostat device. An EGG 273A potentiostat piloted by M352 software was used and connected to the counter electrode composed of a large zinc electrode and to the reference electrode that is a saturated calomel electrode (SCE). All the potentials were given against Hg, $HgCl_2$ / KCl (SCE) electrode.

Cyclic voltametry (CV) was carried out in order to study the deposition mechanism. The potential sweep was applied in the potential range from – 0.8 V/SCE to – 1.8 V/SCE with the scan rate of 20 mV/s. The influence of the variation of deposition conditions like R = Zn(II)/Fe(II) corresponding to the concentration ratio between metallic species and temperature was evaluated. In this study, deposits were realized in galvanostatic mode. The thicknesses of the coatings were quite constant at around 10 microns.

The various phase structures and chemical forms present in the alloy produce various current peaks. Therefore, a dissolution peak characterizes a peculiar structure and permit to evaluate the nature of the phases present in the alloys.

The coating morphology, in topography, and composition modes, was observed using a JEOL JSM-54 device at different magnification. Cross-section observations were also performed in order to evaluate the

* amiratsam@yahoo.fr

quality of the films. Microstructure of the deposited coatings was evaluated using XRD analysis with a Bruker AXS D8 advanced diffractometer in $\theta / 2\theta$ mode in the range of 10-100 ° with a step of 0.02 °.

3. RESULTS AND DISCUSSION

3.1 Electrochemical Characterization

Fig. 1 presents the cyclic polarization curves at 25 °C performed on steel substrate in electrolytic bath. The cyclic diagram shows different cathodic reactions. Between – 0.8 V/SCE and – 0.9 V/SCE, the current density is quite constant and corresponds to the reduction of the dissolved oxygen naturally present in an aerated and stirred electrolytic bath [20].

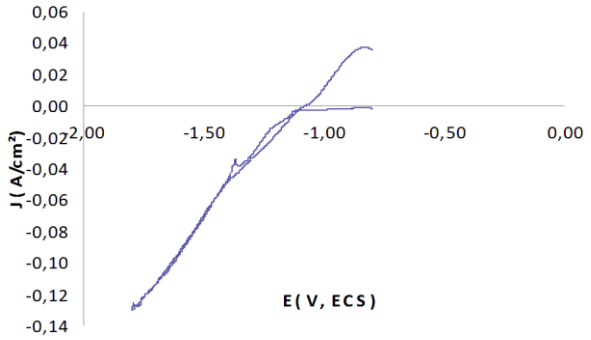

Fig. 1 – Cyclic polarization curves performed on steel surface in the electrolytic bath: for $R = 1/3$ at 20 mV/s

3.2 Study of Early Stages of Electrodeposition of Zn-Fe by Chronoamperometry

Approximately – 1.14 V/SCE, an increase in current density is observed. In the cathode area between: – 1.14 and – 128 V/ECS two different tracks are distinct in the evolution of the current density relative to potential. Two reduction mechanisms associated with metal species may occur.Nucleation and growth are important in the process of electrodeposition of metals. The competition between nucleation and growth determines the size of the deposited metal. The overall appearance and structure of the deposit shall be determined by the shape of the crystal growth.

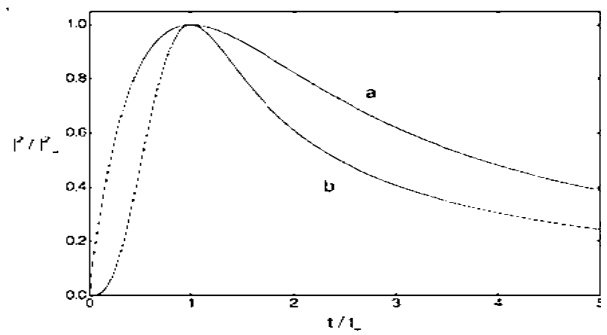

Fig. 2 – Sharifker-Hills Model: dimensionless function; $I^2 / I_m^2 = f(t / t_m)$: (a) – instantaneous and (b) – progressive nucleation

Transitional I (t) normalized to have summers I^2 / I_m^2 versus t / t_m and then compared with those predicted by the well-known theory Sharifker and Hills (Fig. 2).

The plotted curve in Fig. 3 shows clearly that Zn-Fe electrocrystallisaion follows a theoretical response to an instantaneous nucleation in the potential ranges from – 1.17 V to – 1.30 V/ECS. Beyond, this the nucleation changes to a progressive nucleation (Fig. 4).

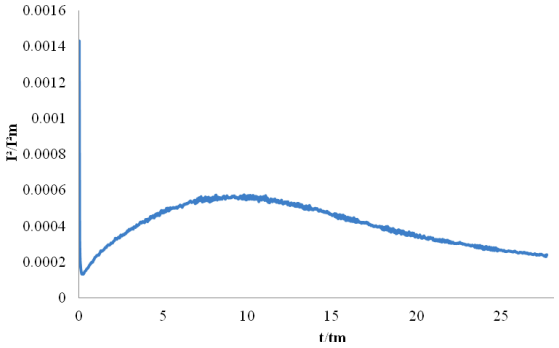

Fig. 3 – Sharifker-Hills Model: Dimensionless function $I^2 / I_m^2 = f(t / t_m)$ for the formation of Zn-Fe: $R = 1/3$, $E = -1.17$ V/ECS

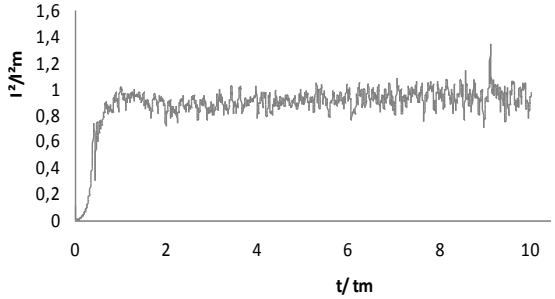

Fig. 4 – Sharifker-Hills Model: Dimensionless function $I^2 / I_m^2 = f(t / t_m)$ for the formation of Zn-Fe: $R = 1/3$, $E = -1.30$ V/ECS

3.3 Morphological and Structural Properties

Morphological observations are used to study the surface topography and to have a glimpse of the co-deposition methods. SEM observations (Fig. 5) for $R = 1/3$ show that the higher the current density the finer are the crystals. The XRD spectra of the Zn-Fe alloy in the range of current densities (10-50 mA/cm²) are presented in Fig. 7. All coatings obtained at low current densities are composed of a mixture of pure hcp – (η)Zn and $FeZn_{13}$ phase (ζ phase has a content of iron about 5-6 weight).

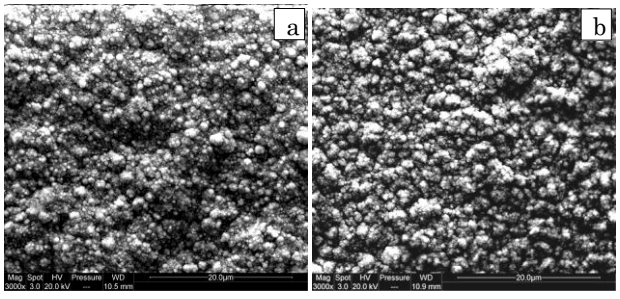

Fig. 5 – SEM micrographs of Zn-Fe deposits for $R = 1/3$, $j = 10$ mA/cm²(a) and $j = 50$ mA/cm² (b)

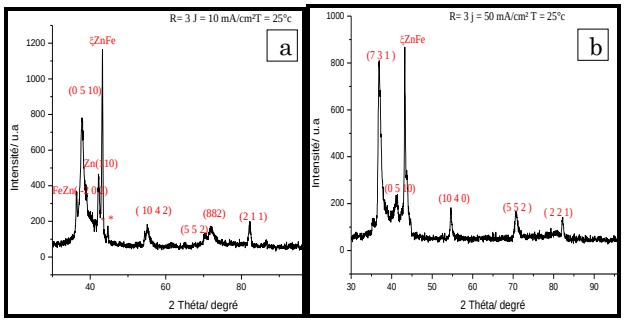

Fig. 6 – X-ray diffraction spectra of Zn-Fe deposits for R = 1/3, j = 10 mA/cm² (a) and j = 50 mA/cm² (b)

4. CONCLUSION

The electrodeposition potential has constant plot transients depending on the model of Sharifker and Hills. The electrocrystallisation of Zn-Fe alloy occurs via instantaneous nucleation with multiple 3D growth controlled by diffusion. SEM observations deposits obtained revealed the diversity of their morphology as a result of their mode of germination and growth. XRD showed that the alloys contain the following phases obtained by the electrolysis conditions: ζ-Zn-Fe and Zn-η. These results are correlated with measures of_ALSV technique.

REFERENCES

1. K.R. Baldwin, M.J. Robinson, C.J.E. Smith, *Cor. Sci.* **35**, 1267 (1993).
2. K.R. Baldwin, M.J. Robinson, C.J.E. Smith, *Br. Cor. J.* **29**, 299 (1994).
3. G. Barcelo, J. Garcia, M. Sarret, C. Muller, J. Pregonas, *J. Appl. Electrochem.* **24**, 1249 (1994).
4. G. Roventi, R. Fratesi, R.A. Della Guardia, G. Barucca, *Appl. Electrochem*. **30**, 173 (2000).
5. D. Sylla, J. Creus, C. Savall, O. Roggy, M. Gadouleau, Ph. Refait, *Thin Solid Films* **424**, 171 (2003).
6. T. Iwagishi, K. Sawada, H. Yamamoto, K. Kojama, H. Shirai, *Electrochemistry* **71**, 318 (2003).
7. D. Sylla, C. Rebere, M. Gadouleau, C. Savall, J. Creus, Ph. Refait, *J. Appl. Electrochem*. **35**, 1133 (2005).
8. D. Sylla, C. Savall, M. Gadouleau, C. Rebere, J. Creus, Ph. Refait, *Surf. Coat. Technol*. **200**, 2137 (2005).
9. C. Savall, C. Rebere, D. Sylla, M. Gadouleau, Ph. Refait, J. Creus, *Mater. Sci. Eng*. A **430**, 165 (2006).
10. Z. Zhang, W.H. Leng, H.B. Shao, J.Q. Zhang, J.M. Wang, C.N. Cao, *J. Electroanal Chem*. **516**, 127 (2001).
11. Z.N. Yang, Z. Zhang, J.D. Zhang, *Surf. Coat. Technol*. **200**, 4810 (2006).
12. N. Lebozec, N. Blandin, D. Thierry, *Mater. Corros.* **59**, 889 (2008).
13. J.J. Sunol, J.J. Fort, *Int. Rev. Phys.* **2**, 31(2008).
14. M. Rezaee Rokn-Abadi, M. Behdani, H. Arabshahi, N. Hosseini, *Int. Rev. Phys*. **32**, 219 (2009).
15. M. Ferhat, *Int. Rev. Phys*. **3**, 190 (2009).
16. M. Zadam, J.A. Adamczyk, A. Tricoteaux, N. Horny, P.Y. Jouan, M.A. Djouadi, M.Y. Debili, *Int. Rev. Phys.* **2**, 426 (2008).
17. V. Narasimhamurthy, B.S. Sheshadri, *Plat. Surf. Finish*. **83**, 75 (1996).
18. J. Bajat, V.B. Miskovic-Stankovic, M.D. Maksimovic, D.M. Drazic, S. Zec, *J. Serb. Chem. Soc*. **69**, 807 (2004).
19. E. Budevski, G. Staikov, W.J. Lorenz, *Electrochim. Acta*, **45**, 4047 (2000).
20. S. Amirat, R. Rehamnia, M. Bordes, J. Creus, *Mater. Corrosion* **62**, 328 (2011).